Int. J. Heat Mass Transfer. Vol. 31, No. 5, pp. 1023–1034, 1988
Printed in Great Britain

0017–9310/88 $3.00 + 0.00

Theory of laminar flame propagation in off-stoichiometric dilute sprays

T. H. LIN
Northwestern University, Evanston, IL 60201, U.S.A.

C. K. LAW
Department of Mechanical Engineering, University of California, Davis, CA 95616, U.S.A.

and

S. H. CHUNG
Seoul National University, Seoul, Korea

(*Received* 3 *June* 1986 *and in final form* 7 *October* 1987)

Abstract—The structure and propagation of a steady, one-dimensional planar, low-speed flame in a dilute, monodisperse, sufficiently off-stoichiometric and weakly-heterogeneous spray, with bulk gas-phase burning, upstream droplet vaporization and downstream droplet vaporization/combustion, is analyzed using activation energy asymptotics. A prevaporized mode and a partially prevaporized mode of flame propagation are identified. Results show that lean and rich sprays exhibit qualitatively opposite behavior in response to the extent of mixture heterogeneity; specifically, the burning intensities of lean and rich sprays are respectively reduced and enhanced with increasing liquid fuel loading and increasing initial droplet size. Classification of all possible spray burning modes as a function of the mixture stoichiometry and initial droplet size is also presented.

1. INTRODUCTION

EXTENSIVE theoretical efforts [1] have been expended at determining the structure and propagation speed of a one-dimensional planar laminar flame in a premixed combustible mixture. The activity has recently reached maturity, at least for simplified kinetics, in that the problem can be solved with mathematical rigor by using large activation energy matched asymptotic analysis.

The corresponding problem of laminar flame propagation in the two-phase medium of a spray is more involved and consequently less well developed. Williams [1] analyzed the limiting situation of heterogeneous flame propagation, in which fuel prevaporization is suppressed such that flame propagation is solely supported by the diffusional burning of droplets. An explicit expression is derived for the heterogeneous flame speed S'_L which is shown to vary inversely with the initial droplet diameter $d'_{-\infty}$. This result is physically realistic in that finer atomization increases the total surface area of all the droplets and consequently the heat release rate.

The heterogeneous flame theory does not allow for any upstream vaporization and thereby the occurrence of bulk gas-phase burning. It is clear that for sufficiently volatile fuels and/or sufficiently small droplets, upstream vaporization is important and the subsequent bulk gas-phase burning could well dominate the flame behavior.

In view of the above considerations, we have formulated a flame propagation theory in dilute sprays, allowing for droplet pre- and post-vaporization, droplet diffusional burning, and premixed burning in the bulk gaseous medium. In the next section we shall first present a systematic classification of all possible modes of combustion depending on the initial droplet size and concentrations of the various reactants in both the gas and liquid phases. In Sections 3 and 4 analysis and results for sufficiently off-stoichiometric lean and rich sprays will be presented. The flame response of near-stoichiometric mixtures is quite complex that a separate study is needed.

The mathematical technique used is matched asymptotic analysis in the limit of large activation energy. We shall also restrict our analysis to dilute sprays in which the mass fraction of the liquid fuel in the fresh mixture is very small [2].

2. CLASSIFICATION OF COMBUSTION MODES

We study the steady, one-dimensional planar, low-speed flame propagation into a combustible mixture consisting of various concentrations of oxidizer, inert, fuel vapor, and fuel droplets of a certain radius. Because of the doubly-infinite nature of the flow configuration, the problem can be studied in a flame-stationary coordinate with the thin reaction zone of the premixed flame being fixed at $x' = 0$ (Fig. 1).

NOMENCLATURE

Dimensional quantities

B'	frequency factor
c_l'	specific heat of liquid fuel
c_p'	specific heat of gas
E_a'	activation energy
F'	mass flux
l'	characteristic preheat zone thickness, $\lambda'/c_p'F'$
L'	specific heat of vaporization
n'	number density
p'	pressure
Q'	heat of combustion per unit mass of fuel
r'	radius of droplet
r_{cr}'	droplet radius for completing vaporization at the flame
r_{st}'	droplet radius for producing stoichiometric burning at the flame
R'	universal gas constant
T'	temperature
u'	flow velocity
W'	molecular weight
$\bar{W}'$	average molecular weight
x'	coordinate
λ'	thermal conductivity
ν'	stoichiometric coefficient
ρ'	density.

Non-dimensional quantities

L	L'/Q'
t	temperature perturbation in inner zone
T	$c_p'T'/Q'$
T_a	activation temperature
x	transformed coordinate, x'/l_T'
y	mass fraction perturbation in inner zone
Y	$Y_F = \tilde{Y}_F$ and $Y_O = \tilde{Y}_O/\sigma$
$\tilde{Y}$	original species mass fraction
Z	ρ_g'/ρ'.

Greek symbols

α	$\alpha = 1$ and 0 in L–L and R–R sprays
γ	$(1-Z_{-\infty})/\varepsilon$
ε	small expansion parameter, T_f^2/T_a
ζ	$(1-Z)/(1-Z_{-\infty})$
Λ	flame speed eigenvalue, equation (15)
ξ	stretched inner variable
σ	stoichiometric ratio
ϕ	equivalence ratio
Ω	initial liquid fuel/initial total fuel.

Superscripts

$\pm$	outer zones on the downstream and upstream sides of the flame front
$'$	dimensional quantities.

Subscripts

b	boiling state
e	state at which droplet is completely gasified
f	flame front
F, O	fuel and oxygen
g, l	gas and liquid phases
i	i = F and O in L–L and R–R sprays
j	j = O and F in L–L and R–R sprays
v	state at which vaporization initiates
in, out	inner and outer zones
0, 1	zeroth and first orders
$-\infty, \infty$	initial and final states.

The structure of the spray flame can be discussed in terms of two groups of parameters. The first group mainly consists of r_{cr}', which is the critical initial droplet radius for the droplet to achieve complete vaporization at the premixed flame front. Thus for $r' < r_{cr}'$ and $r' > r_{cr}'$ we have respectively completely prevaporized burning and partially prevaporized burning, as shown in Figs. 1(a) and (b), respectively. In the partially prevaporized cases, the droplets passing through the flame will undergo either burning or vaporization, depending on the availability of the oxidizer in the downstream region. Complete droplet consumption is achieved at x_e'.

The second group of parameters controls the stoichiometry of the two-phase mixture and can be discussed in terms of the parameters ϕ_t, ϕ_g, and ϕ_f, which respectively represent the fuel/oxidizer equivalence ratios based on the total liquid and gaseous fuels in the freestream, only the gaseous fuel in the freestream, and the gaseous fuel in the freestream plus the amount of liquid fuel vaporized before reaching the flame. Based on these parameters, the following burning modes are possible, as classified in Fig. 1 and Table 1.

If the spray is lean based on both the gaseous fuel as well as the total fuel, which we shall designate as a lean–lean (L–L) spray, then we have $1 > \phi_t > \phi_g$. Two sub-cases can be further identified. If the initial droplet size is less than or equal to the critical droplet size, $r_{-\infty}' \leqslant r_{cr}'$, then complete prevaporization is possible such that $1 > \phi_t = \phi_f > \phi_g$ and the combustion involves only the premixed flame as discussed previously. However, for $r_{-\infty}' > r_{cr}'$, then $1 > \phi_t > \phi_f > \phi_g$ and the subsequent combustion is heterogeneous, involving both premixed burning as well as droplet burning.

The second case involves sprays which are slightly lean (SL), as distinguished by SL–SL and SL–St, where St stands for the stoichiometric state. The equivalence ratios now satisfy the relations $1 \geqslant \phi_t > \phi_g$ and $1-\phi_g = O(\varepsilon)$, where $\varepsilon = T_f^2/T_a$ is the

Table 1. Classification of combustion modes in one-dimensional sprays

Spray stoichiometry	Initial state	Flame state	Initial droplet radius	Downstream state
L–L	$1 > \phi_t > \phi_g$	$1 > \phi_t = \phi_f > \phi_g$ $1 > \phi_t > \phi_f > \phi_g$	$r'_{-\infty} \leqslant r'_{cr}$ $r'_{-\infty} > r'_{cr}$	Pure gas Droplet burning
SL–SL (SL–St)	$1 \geqslant \phi_t > \phi_g$ $1-\phi_g = O(\varepsilon)$	$1 \geqslant \phi_t = \phi_f > \phi_g$ $1 \geqslant \phi_t > \phi_f > \phi_g$	$r'_{-\infty} \leqslant r'_{cr}$ $r'_{-\infty} > r'_{cr}$	Pure gas Droplet burning
SL–SR	$\phi_t > 1 > \phi_g$ $\phi_t - 1 = O(\varepsilon)$ $1-\phi_g = O(\varepsilon)$	$\phi_t = \phi_f > 1 > \phi_g$ $\phi_t > \phi_f \geqslant 1 > \phi_g$ $\phi_t > 1 > \phi_f > \phi_g$	$r'_{-\infty} \leqslant r'_{cr}$ $r'_{cr} < r'_{-\infty} \leqslant r'_{st}$ $r'_{-\infty} > r'_{st}$	Pure gas Droplet vaporization Droplet burning and vaporization
SR–SR (St–SR)	$\phi_t > \phi_g \geqslant 1$ $\phi_g - 1 = O(\varepsilon)$	$\phi_t = \phi_f > 1 \geqslant \phi_g$ $\phi_t > \phi_f > 1 \geqslant \phi_g$	$r'_{-\infty} \leqslant r'_{cr}$ $r'_{-\infty} > r'_{cr}$	Pure gas Droplet vaporization
R–R	$\phi_t > \phi_g > 1$	$\phi_t = \phi_f > \phi_g > 1$ $\phi_t > \phi_f > \phi_g > 1$	$r'_{-\infty} \leqslant r'_{cr}$ $r'_{-\infty} > r'_{cr}$	Pure gas Droplet vaporization

small parameter of expansion for the large activation energy reactions of interest to combustion. The qualitative behavior of this case is similar to that of the first case involving L–L sprays, although the mathematical analysis is somewhat more complicated.

The third case provides the transition from lean to rich sprays in that here the initial gaseous mixture is slightly lean (SL) while the overall mixture is slightly rich (SR). Three subcases are possible. First, if $r'_{-\infty} \leqslant r'_{cr}$, then complete prevaporization occurs and the downstream state consists of only the excess fuel vapor. The second subcase covers the droplet size range satisfying $r'_{cr} < r'_{-\infty} \leqslant r'_{st}$, such that stoichiometric burning occurs in the gaseous mixture at the flame at $r'_{-\infty} = r'_{st}$. This leads to the complete consumption of oxidizer at the flame, with the droplets undergoing pure vaporization in the downstream region. Finally, for $r'_{-\infty} > r'_{st}$, some oxidizer is left at the flame such that the droplets will first burn until the oxidizer is completely depleted. Then the droplets will undergo pure vaporization.

The final two cases of SR–SR (or St–SR) and R–R sprays are analogous to their lean counterparts, except now the downstream state consists of fuel vapor and the vaporizing droplets.

As mentioned earlier, in the present study we shall only tackle the sufficiently off-stoichiometric lean–lean (L–L) and rich–rich (R–R) cases.

3. ANALYSIS FOR OFF-STOICHIOMETRIC BURNING

3.1. *Assumptions*

Since we are primarily interested in the effects of stoichiometry and droplet size on the flame behavior, the following assumptions are made in order to facilitate the analysis. Hence we shall assume that the spray is monodisperse and dilute, with the amount of liquid loading being $O(\varepsilon)$ of the total spray mass. The droplet temperature is constant, and its motion is in phase with that of the gas. Furthermore, in order to suppress the cold boundary difficulty related to droplet vaporization, the droplets start to vaporize, at $x' = x'_v$, only when the gas temperature has reached the boiling

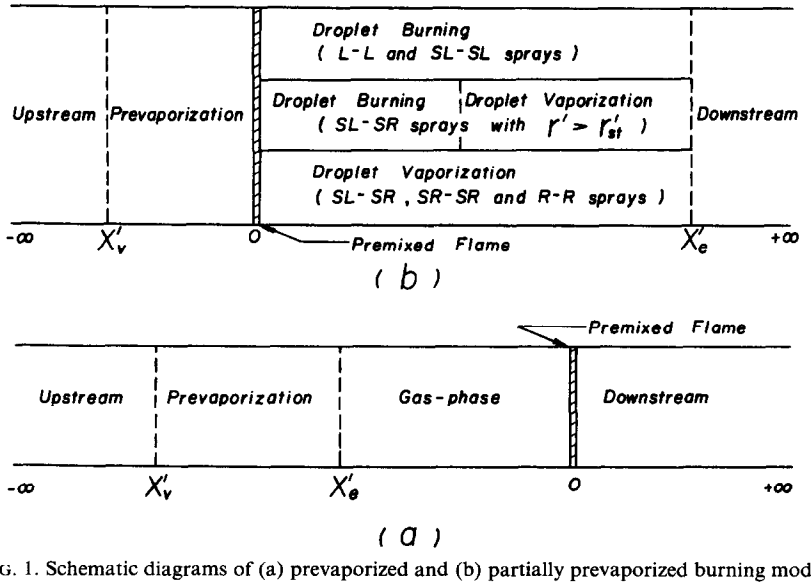

FIG. 1. Schematic diagrams of (a) prevaporized and (b) partially prevaporized burning models.

point of the liquid. Droplets then ignite upon crossing the flame, and will extinguish upon complete depletion of the oxygen in the gas mixture. In the case of R–R sprays only droplet vaporization is possible.

Finally, we assume that the fuel and oxidizer reaction for the bulk premixed flame is one-step overall, that the fuel droplets burn in the flame-sheet limit, and that conventional constant property simplifications apply.

Some additional comments are in order for the present model. First, by assuming the extent of spray heterogeneity as $O(\varepsilon)$, we are excluding phenomena related to the dense spray region near the nozzle exit, where most of the fuel is still in the liquid form while very little air has been entrained. Second, instead of using the droplet spacing or volume ratio to characterize the diluteness of the spray, we use the mass ratio which comes out more naturally from the analysis. Third, the criterion governing initiation of vaporization is a conservative one in that the droplet vaporization rate is usually quite small at such a state. Thus we are able to track the bulk of the vaporization process reasonably well without triggering the cold boundary difficulty. Fourth, the assumption of no slip is made not only for mathematical simplicity and thereby physical clarity in understanding the phenomena of interest, it is also consistent with the dilute spray assumption applicable to regions far away from the injection nozzle, where the initial gas–droplet velocity disparity due to injection has been largely reduced through drag. Fifth, there is also a subtle limitation on the relative amounts of gaseous and liquid fuel present initially. That is, since we assume that droplet ignition is achieved when droplets pass through the premixed flame, the bulk of the fuel must be in the gaseous state at the flame front in order to establish the premixed flame. Thus the model is not capable of describing the highly heterogeneous situation in which the auto-ignition of the droplet is the initiation mode of the spray flame. We shall therefore restrict our study to small values of Ω, defined as the ratio of the initial liquid fuel to the initial total fuel.

3.2. *Governing equations*

The dimensional conservation equations for heat and mass are given in the Appendix. Furthermore, overall continuity of the droplet number density and the total mass respectively requires that

$$n'u' = n'_{-\infty}u'_{-\infty} \tag{1}$$

$$\rho'u' = \rho'_{-\infty}u'_{-\infty} = F' \tag{2}$$

where $\rho' = \rho'_g + (4\pi/3)r'^3 n'\rho'_l$ is the density of the mixture, and $u'_{-\infty}$ is its flame speed, having the same magnitude as S'_L. Quantities with and without primes are dimensional and non-dimensional, respectively.

Following Williams [1], we designate the extent of gas-phase heterogeneity by the parameter $Z = \rho'_g/\rho'$ such that $Z = 1$ represents the completely vaporized state. Then the non-dimensional equations for gas-phase continuity, and conservations of fuel, oxidizer, and energy are respectively given by

$$Z\frac{dZ}{dx} = \frac{A}{T}(1-Z_{-\infty})^{2/3}(1-Z)^{1/3}K(T, Y_O) \tag{3}$$

$$\frac{d}{dx}\left(ZY_F - \frac{d}{dx}Y_F\right) = w + k_F\frac{dZ}{dx} \tag{4}$$

$$\frac{d}{dx}\left(ZY_O - \frac{d}{dx}Y_O\right) = w + k_O\frac{dZ}{dx} \tag{5}$$

$$\frac{d}{dx}\left(ZT - \frac{d}{dx}T\right) = -w + k_T\frac{dZ}{dx} \tag{6}$$

where

$$A = 3\left(\frac{\lambda'}{r'_{-\infty}F'}\right)^2\left(\frac{\rho'\bar{W}'}{R'c'_pQ'\rho'_l}\right)$$

$$w = -\left(\frac{B'\sigma}{W'_O}\right)\left(\frac{p'\bar{W}'}{R'}\right)^2\left(\frac{\lambda'}{c'_pF'^2}\right)Y_OY_F\exp\left(-\frac{T_a}{T}\right)$$

while $x = x'/l'_T$ is the non-dimensional distance expressed in units of the preheat zone thickness $l'_T = \lambda'/(c'_pF')$. In equations (3)–(6), the function $K(T, Y_O)$ and the constant parameters k_F, k_O, and k_T are respectively $\ln[1+(T-T_b-Y_O)/L]$, 0, -1, and $(1-L)$ for the burning droplet and $\ln[1+(T-T_b)/L]$, 1, 0, $-L$ for the vaporizing droplet. In the pure gaseous regions $K(T, Y_O)$ is zero. Also note that quantities related to the droplet size, r', are now expressed through the factor $(1-Z)^{1/3}$.

Finally, we have the ideal gas equation

$$ZT = \left(\frac{p'\bar{W}'c'_p}{R'F'Q'}\right)u'$$

which is used to replace the u' dependence in the gas-phase continuity relation.

For the present problem it is more expedient to use an alternate density parameter [2]

$$\zeta = \frac{1-Z}{1-Z_{-\infty}}$$

instead of Z. Thus in a dilute spray we can expand $Z_{-\infty} = 1-\varepsilon\gamma$ such that $Z = 1-\varepsilon\gamma\zeta$.

3.3. *Outer expansions*

In the broad outer zones, reaction is effectively suppressed because of the temperature-sensitive Arrhenius kinetics. Thus expanding ζ, Y_F, Y_O, and T in terms of ε as

$$\begin{aligned}
\zeta^{\pm}_{out} &= \zeta^{\pm}_0 + \varepsilon\zeta^{\pm}_1 + O(\varepsilon^2)\\
(Y_F)^{\pm}_{out} &= Y^{\pm}_{F0} + \varepsilon Y^{\pm}_{F1} + O(\varepsilon^2)\\
(Y_O)^{\pm}_{out} &= Y^{\pm}_{O0} + \varepsilon Y^{\pm}_{O1} + O(\varepsilon^2)\\
T^{\pm}_{out} &= T^{\pm}_0 + \varepsilon T^{\pm}_1 + O(\varepsilon^2)
\end{aligned} \tag{7}$$

substituting them into equations (3)–(6), and expanding, we have

$$\frac{d\zeta_0^{\pm}}{dx}+\frac{A}{T_0^{\pm}}(\zeta_0^{\pm})^{1/3}K(T_0^{\pm},Y_{O0}^{\pm})+O(\varepsilon^2)=0 \quad (8)$$

$$\left(\frac{d^2Y_{F0}^{\pm}}{dx^2}-\frac{dY_{F0}^{\pm}}{dx}\right)+\varepsilon\left[\frac{d^2Y_{F1}^{\pm}}{dx^2}-\frac{dY_{F1}^{\pm}}{dx}+\gamma\frac{d}{dx}(\zeta_0^{\pm}Y_{F0}^{\pm}-k_F\zeta_0^{\pm})\right]+O(\varepsilon^2)=0 \quad (9)$$

$$\left(\frac{d^2Y_{O0}^{\pm}}{dx^2}-\frac{dY_{O0}^{\pm}}{dx}\right)+\varepsilon\left[\frac{d^2Y_{O1}^{\pm}}{dx^2}-\frac{dY_{O1}^{\pm}}{dx}+\gamma\frac{d}{dx}(\zeta_0^{\pm}Y_{O0}^{\pm}-k_O\zeta_0^{\pm})\right]+O(\varepsilon^2)=0 \quad (10)$$

$$\left(\frac{d^2T_0^{\pm}}{dx^2}-\frac{dT_0^{\pm}}{dx}\right)+\varepsilon\left[\frac{d^2T_1^{\pm}}{dx^2}-\frac{dT_1^{\pm}}{dx}+\gamma\frac{d}{dx}(\zeta_0^{\pm}T_0^{\pm}-k_T\zeta_0^{\pm})\right]+O(\varepsilon^2)=0. \quad (11)$$

3.4. *Inner expansions*

In the inner zone of the bulk gas-phase flame, the solution is expanded around the flame-sheet limit as

$$\begin{aligned}\zeta_{in}&=\zeta_f+O(\varepsilon)\\(Y_F)_{in}&=Y_{Ff}+\varepsilon y_F+O(\varepsilon^2)\\(Y_O)_{in}&=Y_{Of}+\varepsilon y_O+O(\varepsilon^2)\\T_{in}&=T_f+\varepsilon t+O(\varepsilon^2)\end{aligned} \quad (12)$$

with the stretched inner variable being $\xi = x/\varepsilon$.

Substituting equations (12) into equations (3)–(6) and expanding, we have

$$\frac{d\zeta_f}{d\xi}=0 \quad (13)$$

$$\frac{d^2y_F}{d\xi^2}=\frac{d^2y_O}{d\xi^2}=-\frac{d^2t}{d\xi^2}=\frac{\Lambda}{2}(Y_{Ff}+\varepsilon y_F)(Y_{Of}+\varepsilon y_O)e^t \quad (14)$$

where

$$\Lambda=2\left(\frac{T_f^2}{T_a}\right)\left(\frac{B'\sigma}{W_0'}\right)\left(\frac{p'\bar{W}'}{R'}\right)^2\left(\frac{\lambda}{c_p'F'^2}\right)\exp\left(-\frac{T_a}{T_f}\right) \quad (15)$$

is the flame speed eigenvalue.

3.5. *Boundary and jump conditions*

Equations (8)–(11) and (13) and (14) are to be solved subject to the following boundary and jump conditions:

$$x=-\infty:\quad \zeta=1,\quad Y_F=Y_{F,-\infty},\quad Y_O=Y_{O,-\infty},\quad T=T_{-\infty} \quad (16)$$

$$x=x_v:\quad \zeta=1,\quad Y_{F1}^-=Y_{O1}^-=T_1^-=0,\quad T=T_b \quad (17)$$

$$x=x_e\ \text{(prevaporized spray)}:\quad \zeta=0 \quad (18)$$

$$x=0:\quad \zeta=\zeta_f,\quad Y_{F0}^-=Y_{F0}^+,\quad Y_{O0}^-=Y_{O0}^+,\quad T_0^-=T_0^+,\quad Y_{F1}^--Y_{F1}^+=Y_{O1}^--Y_{O1}^+=T_1^+-T_1^- \quad (19)$$

$x = x_e$ (partially prevaporized spray):

$$\zeta=0,\quad Y_F=(1-\alpha)(Y_{j\infty}+\varepsilon\gamma),\quad Y_O=\alpha(Y_{j\infty}-\varepsilon\gamma),\quad T=T_\infty+\varepsilon T_{1\infty} \quad (20)$$

$$x=\infty:\quad \zeta=0,\quad Y_F=(1-\alpha)(Y_{j\infty}+\varepsilon\gamma),\quad Y_O=\alpha(Y_{j\infty}-\varepsilon\gamma),\quad T=T_\infty+\varepsilon T_{1\infty} \quad (21)$$

where, for compactness of notation, we shall use $\alpha = 1$, $i = F$, $j = O$ for lean sprays and $\alpha = 0$, $i = O$, $j = F$ for rich sprays. Furthermore, T_∞ and $T_{1\infty}$ can be determined through energy balance between the far upstream and downstream states

$$T_\infty-T_{-\infty}=Y_{j,-\infty}-Y_{j,\infty}=Y_{i,-\infty} \quad (22)$$

$$T_{1\infty}=\gamma[\alpha-L-(T_\infty-T_b)-(c_l'/c_p')(T_b-T_{-\infty})]. \quad (23)$$

3.6. *Zeroth order solutions*

The zeroth order solution can be readily determined to be

$$\begin{aligned}Y_{F0}^-&=Y_{F,-\infty}-Y_{i,-\infty}e^x,\quad Y_{F0}^+=Y_{Ff}=(1-\alpha)Y_{j,\infty}\\Y_{O0}^-&=Y_{O,-\infty}-Y_{i,-\infty}e^x,\quad Y_{O0}^+=Y_{Of}=\alpha Y_{j,\infty}\\T_0^-&=T_{-\infty}+Y_{i,-\infty}e^x,\quad T_0^+=T_f=T_\infty\end{aligned} \quad (24)$$

which are simply the solutions for the initially premixed gas-phase mixture because of the dilute spray assumption.

Using these relations we find

$$x_v=\ln\left(\frac{T_b-T_{-\infty}}{T_\infty-T_{-\infty}}\right) \quad (25)$$

as well as $\zeta_0^{\pm}$, ζ_f and x_e. That is, for the prevaporized mode, we have

$$(\zeta_0^-)^{2/3}=1-\tfrac{2}{3}A\int_{x_v}^{x}(T_{-\infty}+Y_{i,-\infty}e^x)^{-1}\times\ln\left[1+\frac{(T_{-\infty}-T_b)+Y_{i,-\infty}e^x}{L}\right]dx \quad (26)$$

from which x_e is determined by evaluating equation (26) with $\zeta_0^- = 0$ at $x = x_e$. For the partially prevaporized mode, ζ_0^- is still given by equation (26), while

$$(\zeta_0^+)^{2/3}=\zeta_f^{2/3}-\left(\frac{2}{3}\right)\left(\frac{A}{T_\infty}\right)\times\ln\left[1+\frac{(T_\infty-T_b+\alpha Y_{j,\infty})}{L}\right]x \quad (27)$$

from which x_e is determined by evaluating equation

(27) with $\zeta_0^+ = 0$ at $x = x_e$ while ζ_f is determined by evaluating equation (26) with $\zeta_0^- = \zeta_f$ at $x = 0$.

We now separately present the matching and final solutions for the prevaporized and partially prevaporized modes.

3.7. *Solution for partially prevaporized sprays*

The first order solutions of equations (9)–(11) for this burning mode are given by:

$x_v < x < 0$

$$Y_{F1}^- = a_1(1-e^{x-x_v}) - \gamma e^x \int_{x_v}^{x} [(Y_{F,-\infty}-1)e^{-x} - Y_{i,-\infty}]\zeta_0^- \, dx \quad (28)$$

$$Y_{O1}^- = b_1(1-e^{x-x_v}) - \gamma e^x \int_{x_v}^{x} (Y_{O,-\infty}e^{-x} - Y_{i,-\infty})\zeta_O \, dx \quad (29)$$

$$T_1^- = c_1(1-e^{x-x_v}) - \gamma e^x \int_{x_v}^{x} [(T_{-\infty}+L)e^{-x} + Y_{i,-\infty}]\zeta_0^- \, dx; \quad (30)$$

$0 < x < x_e$

$$Y_{F1}^+ = (1-\alpha)[a_2(1-e^{x-x_e}) + \gamma e^{x-x_e} + \gamma(Y_{j,\infty}-1)e^x \int_x^{x_e} \zeta_0^+ e^{-x} \, dx \quad (31)$$

$$Y_{O1}^+ = \alpha[b_2(1-e^{x-x_e}) - \gamma e^{x-x_e} + \gamma(Y_{j,\infty}+1)e^x \int_x^{x_e} \zeta_0^+ e^{-x} \, dx \quad (32)$$

$$T_1^+ = c_2(1-e^{x-x_e}) + T_{1\infty}e^{x-x_e} + \gamma(T_\infty + L - \alpha)e^x \int_x^{x_e} \zeta_0^+ e^{-x} \, dx \quad (33)$$

where a_1, b_1, c_1, a_2, b_2, and c_2 are determined through matching at the flame.

To perform this matching, we first expand the outer solutions around $x = 0$

$$(Y_F)_{out}^{\pm} = Y_{F0}^{\pm}(0) + \varepsilon\left[Y_{F1}^{\pm}(0) + \frac{dY_{F0}^{\pm}}{dx}(0)\xi\right] + O(\varepsilon^2)$$

$$(Y_O)_{out}^{\pm} = Y_{O0}^{\pm}(0) + \varepsilon\left[Y_{O1}^{\pm}(0) + \frac{dY_{O0}^{\pm}}{dx}(0)\xi\right] + O(\varepsilon^2)$$

$$T_{out}^{\pm} = T_0^{\pm}(0) + \varepsilon\left[T_1^{\pm}(0) + \frac{dT_0^{\pm}}{dx}(0)\xi\right] + O(\varepsilon^2). \quad (34)$$

Then following the detailed matching procedure of ref. [3], we find

$$T_1^+(0) - T_1^-(0) = 0 \quad (35)$$

$$\frac{dT_1^-}{dx}(0) - \frac{dT_1^+}{dx}(0) = \alpha\gamma(1-\zeta_f) - \gamma Y_{i,-\infty} \quad (36)$$

where we have invoked the closure scheme of $Y_{F1}^-(0) = 0$ for lean sprays and $Y_{O1}^-(0) = 0$ for rich sprays.

Using equations (35) and (36), c_1, c_2, $Y_{F1}^{\pm}$, $Y_{O1}^{\pm}$, and $T_1^{\pm}$ can be determined. In particular, we have

$$T_1^+(0) = \left(\frac{1-e^{-x_v}}{e^{-x_e}-e^{-x_v}}\right)\left[T_{1\infty}e^{-x_e} + \gamma(\alpha - Y_{i,-\infty}) \times (1-e^{-x_e}) + \gamma(T_\infty + L - \alpha)\int_0^{x_e} \zeta_0^+ e^{-x} \, dx\right] + \left(\frac{1-e^{-x_e}}{e^{-x_e}-e^{-x_v}}\right)\int_{x_v}^{0} \gamma[(T_{-\infty}+L)e^{-x} + Y_{i,-\infty}]\zeta_0^- \, dx. \quad (37)$$

We note that $T_1^+(0)$ represents the first order downstream temperature perturbation at the flame, and is an important parameter in the present problem.

In the inner zone, application of the local Shvab–Zeldovich formulation to equation (14) yields

$$\frac{d^2}{d\xi^2}(t + y_i) = 0 \quad (38)$$

which has the solution

$$t + y_i = T_1^+(0) \quad (39)$$

satisfying matching conditions (19) and (34).

Integrating energy equation (14), and using equation (39), we obtain

$$\left(\frac{dt}{d\xi}\right)^2 = \left[\Lambda\left(\frac{T_\infty^2}{T_a}\right)Y_{j,\infty}\right][t - T_1^+(0) - 1]e^\theta + d_1. \quad (40)$$

Finally, by applying the matching conditions at $\xi \to \pm\infty$, we find

$$(Y_{i,-\infty})^2 = \left[\Lambda\left(\frac{T_\infty^2}{T_a}\right)Y_{j,\infty}\right]\exp[T_1^+(0)] \quad (41)$$

from which the flame speed S_L', which is built into the definition of Λ, is determined.

The flame speed expression, equation (41), is identical to that of the totally gaseous mixture except for the last term $\exp[T_1^+(0)]$, which therefore represents effects due to droplet processes. In particular, the influence of the initial droplet size appears in the parameter A which is contained in the ζ_0^- and ζ_0^+ terms of $T_1^+(0)$. For the critical state at which the droplets are just completely vaporized at the flame, we have $x_e = 0$, yielding

$$T_1^+(0) = T_{1\infty}. \quad (42)$$

3.8. *Solution for prevaporized sprays*

Following the same procedure as that for the partially prevaporized spray, the outer solutions are now given by

$x_v < x < x_e$

$$Y_{F1}^- = a_3(1-e^{x-x_v}) - \gamma e^x \int_{x_v}^{x} [(Y_{F,-\infty}-1)e^{-x} - Y_{i,-\infty}]\zeta_0^- \, dx \quad (43)$$

$$Y_{O1}^- = b_3(1-e^{x-x_v}) - \gamma e^x \int_{x_v}^{x} (Y_{O,-\infty}e^{-x} - Y_{i,-\infty})\zeta_0^- \, dx \quad (44)$$

$$T_1^- = c_3(1-e^{x-x_v}) - \gamma e^x \int_{x_v}^{x} [(T_{-\infty}+L)e^{-x} + Y_{i,-\infty}]\zeta_0^- \, dx; \quad (45)$$

$x_e < x < 0$

$$Y_{F1}^- = a_4 + a_5 e^x \quad (46)$$

$$Y_{O1}^- = b_4 + b_5 e^x \quad (47)$$

$$T_1^- = c_4 + c_5 e^x. \quad (48)$$

The integration constants in equations (43)–(48) can all be determined from boundary and matching conditions. Solution for the inner zone proceeds analogously with that of the partially prevaporized spray, yielding

$$(Y_{i,-\infty})^2 = \left[\Lambda\left(\frac{T_\infty^2}{T_a}\right)Y_{i,\infty}\right]\exp(T_{1\infty}). \quad (49)$$

It is of interest to note that in the completely prevaporized case $T_1^+(0) = T_{1\infty}$, implying that the flame speed is independent of the initial droplet size of the spray.

4. RESULTS AND DISCUSSIONS

The behavior of the flame propagation speed in a dilute spray, given by equations (41) and (49), has been investigated for both the lean and rich sprays. Transition between the prevaporized and partially prevaporized modes occurs when droplet vaporization is completed just at the flame. Sample calculations are conducted for n-octane (C_8H_{18}) burning in air with $p' = 1$ atm, $\rho_l' = 0.703$ g cm^{-3}, $T'_{-\infty} = 348.6$ K, $T_b' = 398.6$ K, $L' = 71.7$ cal g^{-1}, $Q' = 10.7$ kcal g^{-1}, $\lambda' = 3.47\times10^{-4}$ cal cm^{-1} s^{-1} K^{-1}, $c_p' = 0.397$ cal g^{-1} K^{-1}, and $E_a'/R' = 20\,000$ K. The frequency factor $B' = 10^{10}$ cm^3 mol^{-1} s^{-1} is fixed by matching the calculated and experimental flame speeds in the homogeneous limit. We also use Ω to indicate the ratio of the liquid fuel to the total fuel in the initial state.

4.1. *The flame speed*

Figure 2 plots the variations of $S_L'/\exp[T_1^+(0)/2]$ with Ω and ϕ_t. Since the dependence of S_L' on the droplet size is through $T_1^+(0)$, such a plot isolates the dependence of S_L' to effects caused only by gas-phase burning. Noting that the gas-phase fuel concentration is reduced with fuel in the liquid state, this leaning effect of gas-phase burning results in a lower flame

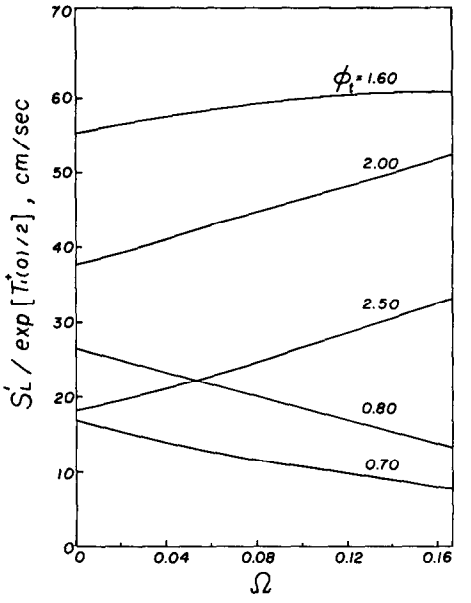

FIG. 2. Variations of $S_L'/\exp[T_1^+(0)/2]$ with the mass fraction of liquid fuel Ω and the equivalence ratio based on total fuel ϕ_t.

temperature and flame speed in the lean spray but a higher flame temperature and flame speed in the rich spray. The more the liquid fuel, corresponding to larger values of Ω, the greater is the respective effect on flame weakening and intensification.

Figure 3 shows the dependence of the flame temperature perturbation $T_1^+(0)$ on the initial droplet size. It is seen that each of these curves consists of a flat segment corresponding to the completely prevaporized mode, and a monotonically varying segment corresponding to the partially prevaporized mode. As $r'_{-\infty} \to 0$, the present analysis breaks down because small droplets can start to vaporize from the far upstream state, thereby contradicting the assumption of a finite x_v here.

Results of Fig. 3 can be explained as follows. For a lean spray, the liquid fuel absorbs heat for upstream vaporization, produces the secondary gasified fuel for the bulk gas-phase burning, burns through droplet combustion afterwards, and finally results in a positive $T_1^+(0)$. On the other hand the secondary gasified fuel in a rich spray is equivalent to an inert without any contribution to burning, thereby producing a negative $T_1^+(0)$.

Furthermore, since in the prevaporized mode the fuel concentration near the flame is the same as that of a gaseous premixture, $T_1^+(0)$ depends only on ϕ_t and Ω but not on the initial droplet size. Increasing the mass fraction of the liquid fuel, Ω, increases the magnitude of $T_1^+(0)$ because in rich sprays higher values of Ω result in a larger amount of heat absorption due to droplet vaporization, which causes correspondingly larger reductions in $T_1^+(0)$. On the other hand, in lean sprays the heat absorption due to vaporization is much smaller than the correspond-

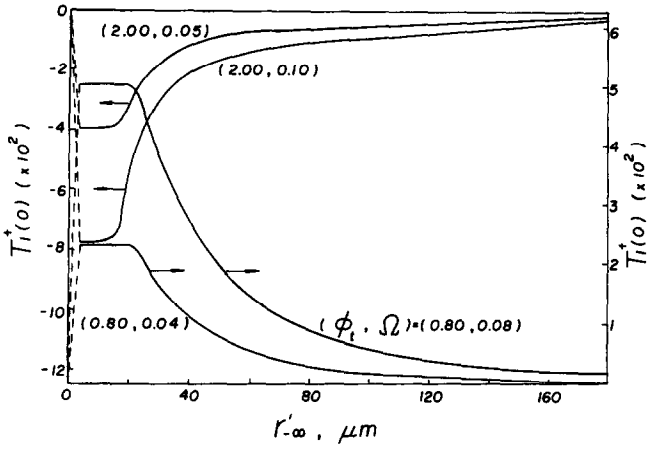

FIG. 3. Variations of flame temperature perturbation $T_1^+(0)$ with the initial droplet size $r'_{-\infty}$ and the mass fraction of liquid fuel Ω.

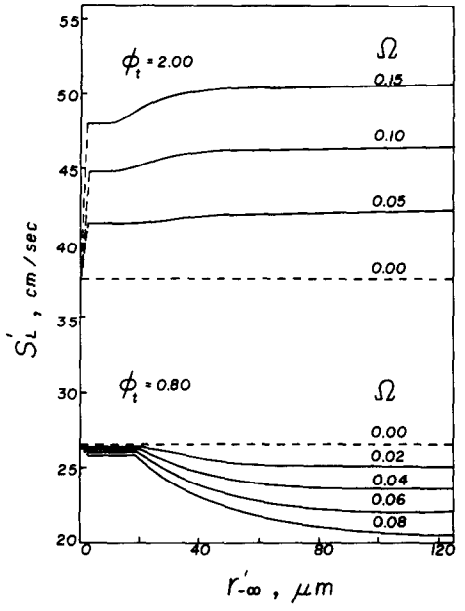

FIG. 4. Flame speed S'_L as functions of the initial droplet size $r'_{-\infty}$ and the mass fraction of liquid fuel Ω.

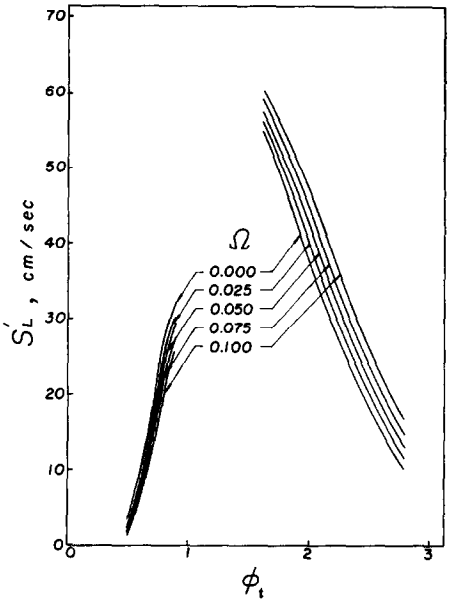

FIG. 5. Flame speed S'_L vs the total equivalence ratio ϕ_t on constant mass fraction of liquid fuel Ω ($r'_{-\infty} = 50$ μm).

ingly increased combustion heat release due to the additional secondary gasified fuel. Thus larger values of Ω result in stronger burning intensities with higher positive values of $T_1^+(0)$.

Concerning the influence of the droplet size, we note that in the partially prevaporized mode, a lean spray containing larger droplets has a slower gasification rate and therefore less secondary gasified fuel near the flame, resulting in smaller values of $T_1^+(0)$. On the other hand larger droplets in a rich spray will render the gas mixture less fuel rich and thereby reduce the negative effect of fuel vaporization on $T_1^+(0)$.

Combining results of Figs. 2 and 3, the flame speed S'_L is shown in Fig. 4 for different values of $r'_{-\infty}$ and Ω. It is seen that the flame speed of a lean spray, $\phi_t = 0.80$, is lower than the corresponding gaseous premixture. It is further weakened with increasing initial droplet size for the partially prevaporized mode. The converse holds for the rich spray.

Figures 5 and 6 show the conventional plots of the flame speed vs the (total) equivalence ratio on constant Ω and $r'_{-\infty}$, respectively. Since the analysis is only valid for sufficiently off-stoichiometric mixtures, a continuous transition from lean-to-rich burning cannot be obtained here. Figure 6 shows the interesting result that curves of different $r'_{-\infty}$ converge with decreasing ϕ_t because of the reduction of the net amount of liquid fuel initially present in the mixture. Furthermore, for the same reason which is responsible for the behavior of $T_1^+(0)$ as discussed above, larger droplets reduce the flame speed in a lean spray and increase the flame speed in a rich spray.

4.2. *Temperature and concentration profiles*

Figures 7 and 8 show the profiles for the zeroth order temperature (T_0), fuel mass fraction (Y_{F0}), and

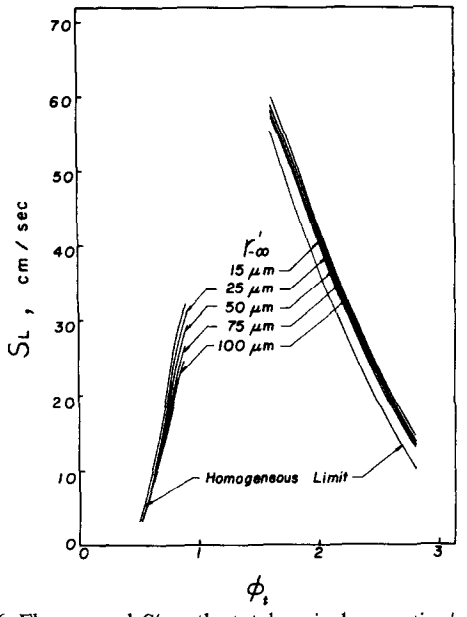

FIG. 6. Flame speed S'_L vs the total equivalence ratio ϕ_t on constant initial droplet size $r'_{-\infty}$ ($\Omega = 0.05$).

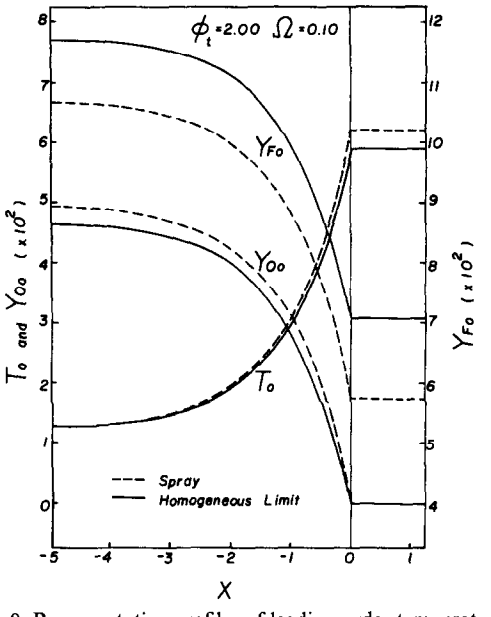

FIG. 8. Representative profiles of leading order temperature T_0, fuel vapor concentration Y_{F0}, and oxygen concentration Y_{O0} in a rich spray.

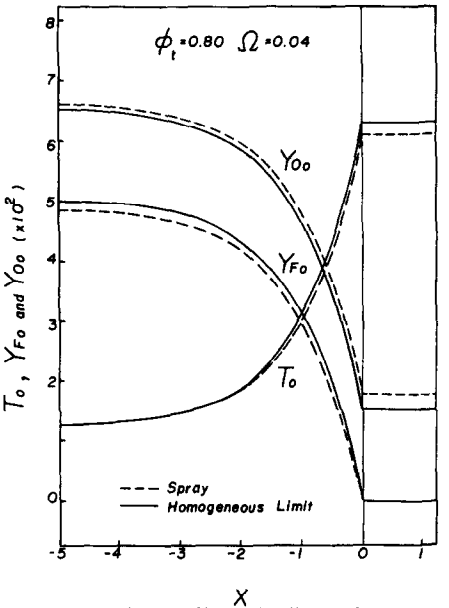

FIG. 7. Representative profiles of leading order temperature T_0, fuel vapor concentration Y_{F0}, and oxygen concentration Y_{O0} in a lean spray.

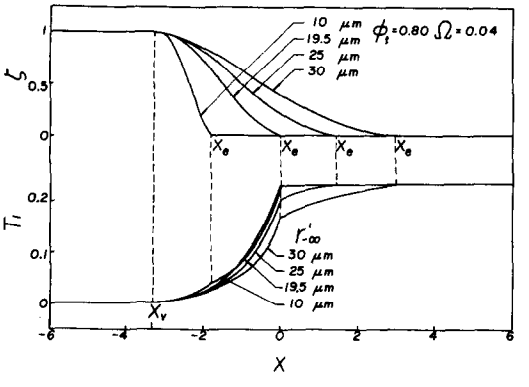

FIG. 9. Representative profiles of spray heterogeneity parameter ζ and temperature perturbation T_1 in a lean spray.

oxygen mass fraction (Y_{O0}), respectively. Since heterogeneity does not affect the leading order solutions because of the dilute spray assumption, the differences between the solutions of the homogeneous mixture and the spray are due to the diversion of some of the gaseous fuel to the liquid fuel in the initial state, which leads to different flame temperatures.

Figures 9 and 10 show profiles of ζ, T_1, Y_{F1} and Y_{O1} in a lean spray with different initial droplet size. It is seen that the density parameter of the liquid fuel, ζ, remains at the initial state before reaching x_v, and

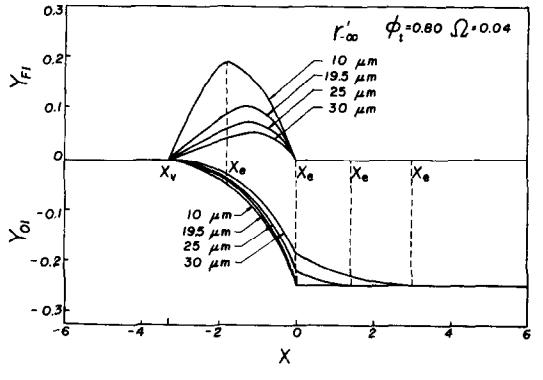

FIG. 10. Representative profiles of perturbations of fuel vapor concentration Y_{F1} and oxygen concentration Y_{O1} in a lean spray.

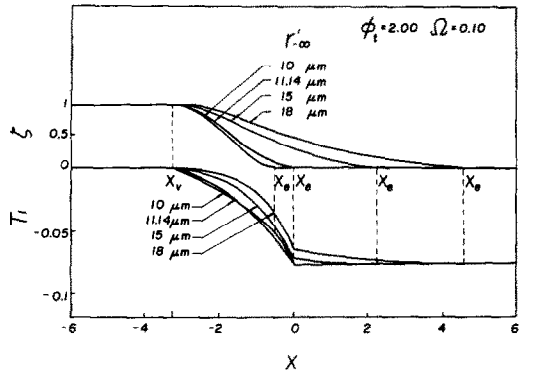

FIG. 11. Representative profiles of spray heterogeneity parameter ζ and temperature perturbation T_1 in a rich spray.

vanishes at x_e upon total droplet consumption. The influence of heterogeneity on T_1 is two-fold, namely prevaporization should lower the gas temperature while consumption of this additional, prevaporized fuel should elevate the gas temperature. It is seen that the latter has a stronger effect in that small droplets lead to higher T_1 because of the faster vaporization upstream of the flame as well as faster combustion downstream of the flame.

The Y_{F1} results of Fig. 10 show competing effects of the production and consumption of the secondary gasified fuel, which lead to the existence of a maximum concentration somewhere upstream of the flame. Finally, the Y_{O1} profiles show the dilution effect on the oxygen mass fraction by the secondary gasified fuel upstream, and the consumption of oxygen through droplet burning downstream.

Figures 11 and 12 show the corresponding profiles of ζ, T_1, Y_{F1} and Y_{O1} for a rich spray. The behavior can all be adequately explained on the basis of the further enrichment of an already rich spray through droplet vaporization. In particular, Fig. 12 shows that Y_{O1} exhibits a minimum-point behavior, caused by the initial continuous dilution of the oxygen concentration through fuel vaporization, and the subsequent complete consumption of the oxygen at the flame.

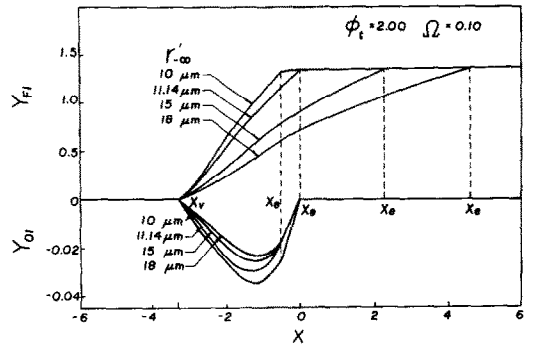

FIG. 12. Representative profiles of perturbations of fuel vapor concentration Y_{F1} and oxygen concentration Y_{O1} in a rich spray.

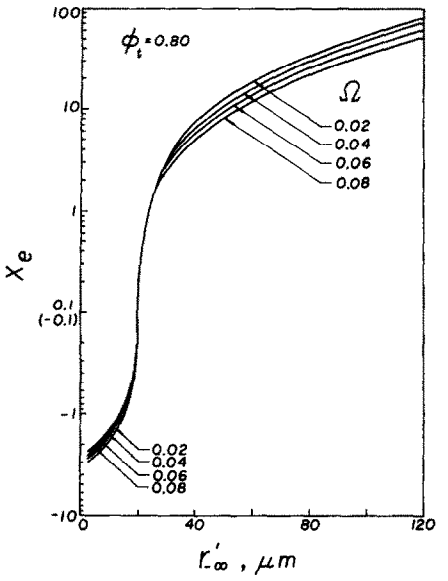

FIG. 13. Dependence of the location x_e on the initial droplet size $r'_{-\infty}$ and mass fraction of liquid fuel Ω for a lean spray.

4.3. *State of complete droplet consumption*

The state of complete droplet consumption, x_e, is an important parameter in the present problem because it indicates whether complete prevaporization is possible and, if it is not, how much longer would it require to recover all the chemical heat release through droplet burning in the case of a lean spray. Figures 13 and 14 show x_e for lean and rich sprays, respectively. It is seen that complete prevaporization ($x_e \leqslant 0$) can be achieved for initial droplet sizes around 10–20 μm. The distance over which this complete prevaporization can be achieved is $x_e = O(1)$. Since the physical distance x' is scaled by the characteristic preheat zone thickness l'_T, this result then implies that

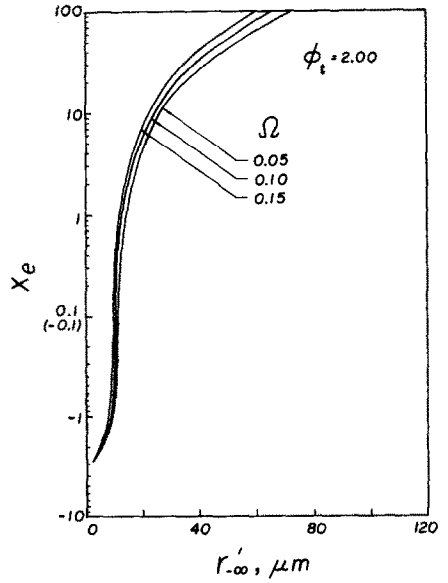

FIG. 14. Dependence of the location x_e on the initial droplet size $r'_{-\infty}$ and mass fraction of liquid fuel Ω for a rich spray.

the bulk of the prevaporization occurs in the preheat zone, as is reasonable to expect. Results further show that for droplets exceeding 20 μm such that complete prevaporization cannot be achieved, substantially longer x_c is required for larger droplets because a correspondingly larger amount of droplet mass is involved.

4.4. *Comparisons*

There are several sources of theoretical and experimental information with which the present study can be compared. First, Ballal and Lefebvre [4] have experimentally observed that for overall lean and stoichiometric sprays, the flame speed decreases with increasing liquid fuel loading and increasing droplet size. Hayashi and Kumagai [5] also reported that the flame speed decreases with increasing liquid fuel loading for lean sprays but increases for rich sprays. Since both of these works use low values of Ω, which is the situation studied herein, the agreement is reasonable.

Hayashi *et al.* [6], however, have further observed that the flame speed also increases with increasing droplet size, even for an overall fuel-lean mixture, provided the droplet is sufficiently large. Such an effect is attributed [6] to the observed heterogeneity-induced wrinkling of the flame surface.

Polymeropoulos [7] and Polymeropoulos and Das [8] have theoretically and experimentally shown the existence of an optimum droplet size at which the flame speed attains a maximum value. This is contrary to the present monotonic behavior. It is believed that the reason for the disagreement is that the sprays of refs. [7, 8] are highly heterogeneous while the present study is restricted to low levels of heterogeneity. Thus the transition from the heterogeneously-dominated to the homogeneously-dominated behavior is not captured here.

Finally, because of further droplet vaporization after the droplets pass through the premixed flame front, Seth *et al.* [9] and Aggarwal and Sirignano [10] have numerically observed either the formation of a diffusion flame downstream of the premixed flame, or the back diffusion of the fuel vapor towards the flame. While it is unclear as to what extent these results are caused by the fact that their model involves unsteady flame propagation in a closed volume, they do suggest the possibility that droplets need not burn via the individual envelope diffusion flame mode (for lean sprays) downstream of the premixed flame front. A more rigorous treatment should incorporate suitable droplet ignition/extinction criteria in this region.

5. CONCLUDING REMARKS

In the present investigation we have studied the flame structure and propagation rate of dilute sprays undergoing sufficiently off-stoichiometric burning. The qualitatively different behavior of lean and rich sprays can all be explained on the basis of the reduction of the gas-phase fuel concentration through mixture heterogeneity such that the burning intensities of lean and rich sprays are respectively reduced and enhanced. Parametrically, the results show that the flame propagation rate of a lean spray increases with decreasing liquid fuel loading and decreasing initial droplet size, while the opposite holds for a rich spray.

It is important to emphasize that much improvement is still needed for the present model. For example, we should relax the assumption of a finite x_v' at which vaporization is initiated so that the theory can specialize to the homogeneous limit of laminar flame propagation in a completely gaseous mixture. Furthermore, in order for the theory to approach the heterogeneous limit also at which the spray flame is entirely supported by droplet burning, and to allow for downstream droplet vaporization and thereby back diffusion of the fuel vapor, it is necessary to use proper droplet ignition/extinction criteria such as those of refs. [11, 12]. This is because the present assumption that the droplets automatically ignite upon crossing the gaseous flame front obviously becomes inoperative either in the heterogeneous limit or for very small droplets. Finally, in order to provide a smooth transition from lean to rich burning, a two-reactant formulation is needed to describe the significant changes in both the fuel and oxidizer concentrations for stoichiometric and near-stoichiometric mixtures.

Acknowledgement—This work was supported by the Heat Transfer Program of NSF under Grant No. MEA 84-15080.

REFERENCES

1. F. A. Williams, *Combustion Theory*. Benjamin–Cummins, Palo Alto, California (1985).
2. T. Mitani, A flame inhibition theory by inert dust and spray, *Combust. Flame* **43,** 243 (1981).
3. S. H. Chung and C. K. Law, Structure and extinction of convective diffusion flames with general Lewis numbers, *Combust. Flame* **52,** 59 (1983).
4. D. R. Ballal and A. H. Lefebvre, Flame propagation in heterogeneous mixtures of fuel droplets, fuel vapor and air, Eighteenth Symposium on Combustion, The Combustion Institute, Pittsburgh, Pennsylvania, p. 321 (1981).
5. S. Hayashi and S. Kumagai, Flame propagation in fuel droplet–vapor–air mixtures, Fifteenth Symposium on Combustion, The Combustion Institute, Pittsburgh, Pennsylvania, p. 445 (1975).
6. S. Hayashi, S. Kumagai and T. Sakai, Propagation velocity and structure of flames in droplet–vapor–air mixtures, *Combust. Sci. Technol.* **15,** 169 (1976).
7. C. E. Polymeropoulos, Flame propagation in a one-dimensional liquid fuel spray, *Combust. Sci. Technol.* **9,** 197 (1974).
8. C. E. Polymeropoulos and S. Das, The effect of droplet size on the burning velocity of kerosene–air sprays, *Combust. Flame* **25,** 247 (1975).
9. B. Seth, S. K. Aggarwal and W. A. Sirignano, Flame propagation through an air–fuel spray mixture with transient droplet vaporization, *Combust. Flame* **39,** 149 (1980).
10. S. K. Aggarwal and W. A. Sirignano, Unsteady spray flame propagation in a closed volume, *Combust. Flame* **62,** 69 (1985).

11. C. K. Law, Asymptotic theory for ignition and extinction in droplet burning, *Combust. Flame* **24**, 89 (1975).
12. C. K. Law, Theory of thermal ignition in fuel droplet burning, *Combust. Flame* **31**, 285 (1978).

APPENDIX: DIMENSIONAL CONSERVATION EQUATIONS

The conservation equations of heat and mass for the present steady-state, one-dimensional, chemically-reacting two-phase flows with phase change are given by:

gas-phase continuity

$$\frac{\mathrm{d}}{\mathrm{d}x'}(\rho_g' u') = K'(T', \tilde{Y}_O);$$

conservation of fuel mass

$$\frac{\mathrm{d}}{\mathrm{d}x'}\left[\rho_g' u' \tilde{Y}_F - (\rho_g' D')_F \frac{\mathrm{d}\tilde{Y}_F}{\mathrm{d}x'}\right] = w' + k_F K'(T', \tilde{Y}_O);$$

conservation of oxidizer mass

$$\frac{\mathrm{d}}{\mathrm{d}x'}\left[\rho_g' u' \tilde{Y}_O - (\rho_g' D')_O \frac{\mathrm{d}\tilde{Y}_O}{\mathrm{d}x}\right] = \sigma w' + k_O \sigma K'(T', \tilde{Y}_O);$$

conservation of energy

$$\frac{\mathrm{d}}{\mathrm{d}x'}\left[\rho_g' u' c_p' T' - \lambda' \frac{\mathrm{d}T'}{\mathrm{d}x'}\right] = -Q' w' + k_T' K'(T', \tilde{Y}_O);$$

ideal gas equation

$$p' \bar{W}' = \rho_g' R' T'$$

where

$$w' = -\frac{B'}{W_0'}\left(\frac{\rho' \bar{W}'}{R'}\right)^2 \tilde{Y}_F \tilde{Y}_O \exp\left(-\frac{E_a'}{R' T'}\right).$$

The function $K'(T', \tilde{Y}_O)$ and the constant parameters k_F, k_O and k_T' are respectively

$$4\pi \frac{\lambda'}{c_p'} n' r' \ln\left[1 + \frac{c_p'(T' - T_b')}{L'} + \frac{(\tilde{Y}_O/\sigma)Q'}{L'}\right],$$

$$0, \quad -1 \text{ and } (Q' - L')$$

for the burning droplet case and

$$4\pi \frac{\lambda'}{c_p'} n' r' \ln\left[1 + \frac{c_p'(T' - T_b')}{L'}\right], \quad 1, \quad 0 \text{ and } -L'$$

for the vaporizing droplet case. In the pure gaseous regions $K'(T', \tilde{Y}_O)$ is zero.

THEORIE DE LA PROPAGATION D'UNE FLAMME LAMINAIRE DANS LES BROUILLARDS DILUES NON STOICHIOMETRIQUE

Résumé—On analyse à partir de l'énergie d'activation asymptotique la structure et la propagation d'une flamme permanente, plane à faible vitesse, dans un brouillard monodispersé, suffisamment hors stoichiométrie, faiblement hétérogène, avec une vaporisation des gouttelettes en avant de la combustion en phase gazeuse. On identifie un mode de prévaporisation et un mode prévaporation partielle pour la propagation de flamme. Les résultats montrent que les brouillards pauvres ou riches montrent des comportements qualitativement opposés; spécifiquement, les intensités de combustion des brouillards pauvres ou riches sont respectivement réduites ou augmentées par un accroissement de la charge en combustible liquide et de la taille initiale des gouttelettes. On présente aussi une classification de tous les modes possibles de combustion des brouillards en fonction de la stoichiométrie du mélange et de la taille initiale des gouttelettes.

THEORIE DER AUSBREITUNG EINER LAMINAREN FLAMME IN EINER NICHT-STÖCHIOMETRISCHEN VERDÜNNTEN SPRÜHSTRÖMUNG

Zusammenfassung—Struktur und Ausbreitung einer stationären, eindimensional ebenen Flamme von geringer Geschwindigkeit in einer verdünnten, monodispersen, ausreichend nicht-stöchiometrischen und leicht heterogenen Sprühströmung wurden analytisch untersucht. Im Kern ist die Gasphase in Brand, stromauf verdampfen Tröpfchen, stromab findet Verdampfung und Verbrennung von Tröpfchen statt. Zwei Arten der Flammenausbreitung wurden gefunden, eine mit vollständiger und eine mit teilweiser Vorverdampfung. Die Ergebnisse zeigen, daß magere und fette Sprühströmungen im Hinblick auf die Gemisch-Heterogenität qualitativ entgegengesetztes Verhalten zeigen. Insbesondere nimmt die Verbrennungs-Intensität der mageren und der fetten Strömung ab bzw. zu, wenn die Brennstoffzufuhr und die anfängliche Tropfengröße erhöht werden. Die möglichen Verbrennungsarten werden abhängig von der Gemisch-Stöchiometrie und der anfänglichen Tropfengröße klassifiziert.

ТЕОРИЯ РАСПРОСТРАНЕНИЯ ЛАМИНАРНОГО ПЛАМЕНИ В НЕСТЕХИОМЕТРИЧЕСКИХ ОБЕДНЕННЫХ ЖИДКИМ ТОПЛИВОМ СТРУЯХ

Аннотация—В работе анализируются с использованием асимптотики энергии активации структура и распространение устойчивого одномерного плоского, низкоскоростного пламени в обедненной монодисперсной нестехиометрической слабогетерогенной струе с горением в объеме газовой фазы, испарение капли в начальной части потока и испарение-горение капли в направлении течения. Определяются доиспарительный и частично доиспарительный режимы распространения пламени. Результаты показывают, что поведение обедненных и насыщенных жидким топливом струй качественно отличаются в зависимости от степени гетерогенности смеси; в частности, интенсивность горения обедненных и насыщенных струй уменьшается и усиливается, соответственно, с увеличением содержания жидкого топлива и увеличением начального размера капли. Также дается классификация возможных режимов струйного горения как функция стехиометрии смеси и начального размера капли.